Response of air-sea carbon fluxes and climate to orbital forcing changes in the Community Climate System Model

M. Jochum,[1] S. Peacock,[1] K. Moore,[2] and K. Lindsay[1]

[1] A global general circulation model coupled to an ocean ecosystem model is used to quantify the response of carbon fluxes and climate to changes in orbital forcing. Compared to the present-day simulation, the simulation with the Earth's orbital parameters from 115,000 years ago features significantly cooler northern high latitudes but only moderately cooler southern high latitudes. This asymmetry is explained by a 30% reduction of the strength of the Atlantic Meridional Overturning Circulation that is caused by an increased Arctic sea ice export and a resulting freshening of the North Atlantic. The strong northern high-latitude cooling and the direct insolation induced tropical warming lead to global shifts in precipitation and winds to the order of 10%–20%. These climate shifts lead to regional differences in air-sea carbon fluxes of the same order. However, the differences in global net air-sea carbon fluxes are small, which is due to several effects, two of which stand out: first, colder sea surface temperature leads to a more effective solubility pump but also to increased sea ice concentration which blocks air-sea exchange, and second, the weakening of Southern Ocean winds that is predicted by some idealized studies occurs only in part of the basin, and is compensated by stronger winds in other parts.

Citation: Jochum, M., S. Peacock, K. Moore, and K. Lindsay (2010), Response of air-sea carbon fluxes and climate to orbital forcing changes in the Community Climate System Model, *Paleoceanography*, *25*, PA3201, doi:10.1029/2009PA001856.

1. Introduction

[2] Over the last 400,000 years Earth's climate went through several glacial and interglacial eras, which are correlated with changes in its orbit and the associated changes in solar insolation [*Milankovitch*, 1941; *Hays et al.*, 1976; *Huybers and Wunsch*, 2004]. Over this time changes in global ice volume, temperature and atmospheric partial pressure of CO_2 (pCO_2) have been strongly correlated with each other [*Petit et al.*, 1999]. The connection between temperature and ice volume is not surprising, and a strong snow/ice-albedo feedback makes it plausible to connect both to changes in the Earth's orbit [*Huybers and Tziperman*, 2008, and references therein]. The magnitude of the pCO_2 variations, however, are still not understood [*Sigman and Boyle*, 2000], and it appears increasingly unlikely that a single process can account for the observed changes [*Sarmiento and Gruber*, 2006, section 10.4].

[3] The motivation of the present study comes from *Peacock et al.* [2006], who, based on the analysis of observations and several box models, suggest a sequence of different processes to explain the observed glacial-interglacial pCO_2 variations. They conclude that the first pCO_2 response to a change in Earth's orbit is likely to be driven by changed mixing and solubility in the Southern Ocean. This dominance of the Southern Ocean pCO_2 response has already been suggested by earlier box models [*Siegenthaler and Wenk*, 1984; *Sarmiento and Toggweiler*, 1984; *Knox and McElroy*, 1984], but their fidelity has been called in question by recent carbon cycle studies with full circulation models [e.g., *Toggweiler et al.*, 2003; *Lane et al.*, 2006]. Thus, given the uncertainty surrounding box models and the importance of the carbon cycle, we decided to reassess the Peacock et al. result with a fully coupled general circulation model (GCM).

[4] GCMs are too computationally expensive to be integrated over a glacial cycle, so the present approach will focus on the differences in the air-sea carbon flux between two simulations with solar insolations based on two different orbits. This approach should be viewed as complementary to box models: box models can be used to arrive at a self-consistent interpretation of the observations, and GCMs can be used to validate assumptions made in box models. Here specifically the GCM will be used to assess if and where the air-sea flux of CO_2 is sensitive to orbital changes. Section 2 describes the GCM and the experimental setup, section 3 describes the results, and section 4 provides summary and discussion.

2. Description of Model and Experiment

[5] The numerical experiment is performed using the National Center for Atmospheric Research (NCAR) Community Climate System Model version 3 (CCSM3), which consists of fully coupled atmosphere, ocean, land and sea ice models; a detailed description can be found in the work by *Collins et al.* [2006].

[1] National Center for Atmospheric Research, Boulder, Colorado, USA.

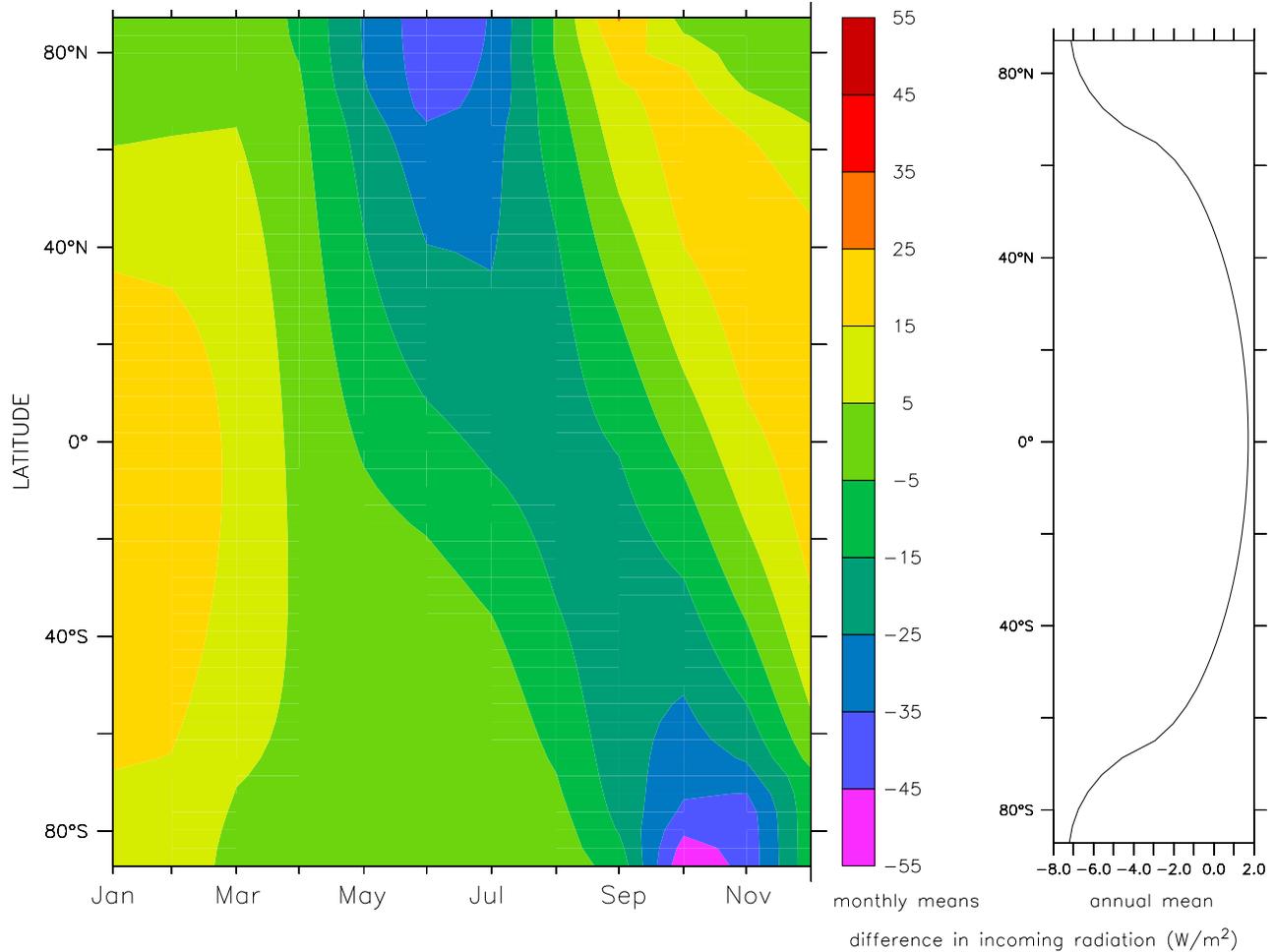[2] Department of Earth System Science, University of California, Irvine, California, USA.

Figure 1. (left) Seasonal cycle and (right) mean differences between CONT and OP115 in solar insolation at the top of the atmosphere (OP115-CONT, in W/m^2).

[6] The ocean model has a zonal resolution that varies from 340 km at the equator to 40 km around Greenland, and a meridional resolution that varies from 70 km at the equator to 40 km around Greenland and 350 km in the North Pacific. This spatially varying resolution is achieved by placing the north pole of the grid over Greenland, and reflects the different relevant length scales of the 2 processes that are deemed most important to maintain a stable global climate: deep convection around Greenland and in the Arctic, and oceanic heat uptake at the equator. In the vertical there are 25 depth levels; the uppermost layer has a thickness of 8 m, the deepest layer has a thickness of 500 m. The atmospheric model uses T31 spectral truncation in the horizontal (about 3.75° resolution) with 26 vertical levels. The sea ice model shares the same horizontal grid as the ocean model and the land model is on the same horizontal grid as the atmosphere. This setup (called T31x3) has been developed specifically for long paleoclimate and biogeochemistry integrations, and its performance is described in detail by *Yeager et al.* [2006]. Compared to this publicly released version, the present version has several modified parameterizations, but the only modification relevant for the present study is an increase of the thermocline diapycnal diffusivity from 0.1 to 0.2 cm^2/s, which is more consistent with observed values (see review by *Jochum* [2009]).

[7] The CCSM biogeochemistry (BEC) model is the result of combining the upper ocean ecosystem model of *Moore et al.* [2001] with the biogeochemistry module of *Doney et al.* [2001]. It includes the nutrients nitrate, ammonium, phosphate, iron, and silicate; four phytoplankton groups, one class of zooplankton, dissolved organic matter, sinking particulate detritus, and it has been extensively tested within CCSM3 [*Moore et al.*, 2004; *Doney et al.*, 2009].

[8] The configuration described above is integrated for 500 years (of which the final 200 years will be used for the analysis, unless noted otherwise) with present-day solar insolation and fixed atmospheric CO_2 (260 ppm), and serves as control (experiment CONT). Experiment OP115 is identical to CONT except for the solar insolation, which is based on Earth's orbital parameters 115,000 years ago (115 kya). This particular time is chosen because the solar forcing at 65°N during June differs from its present value more than during most other epochs [*Berger and Loutre*, 1991], with obliquity and precession differences being about equally
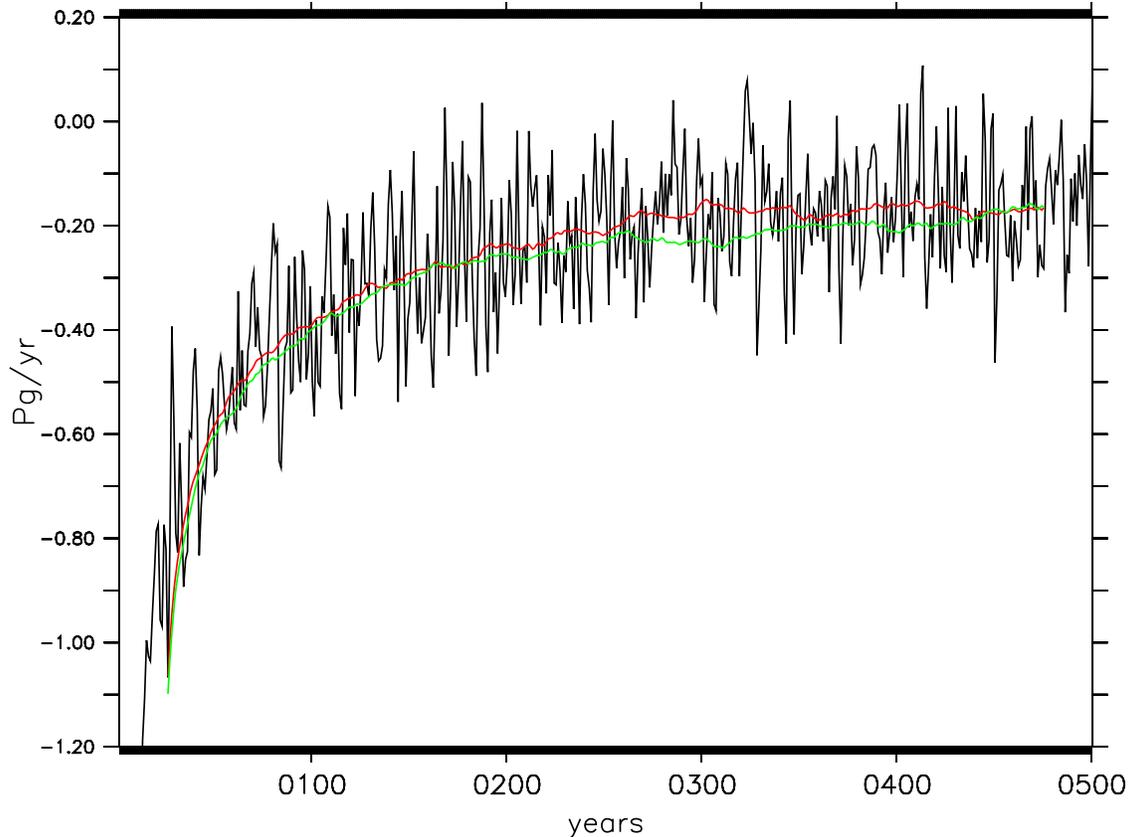
Figure 2. Time evolution of annual mean air-sea carbon fluxes for CONT (black) and the fluxes smoothed with a 50 year boxcar filter for CONT (red) and OP115 (green).

important [*Berger and Pestiaux*, 1984; *Short et al.*, 1991]. In particular at high latitudes there is less insolation during spring and early summer months and more radiation later in the summer. Annual mean insolation is reduced at high latitudes and increased slightly at lower latitudes (Figure 1).

[9] This experimental design is not optimal, and compromised mostly because of the high computational cost of a full GCM with BGC. Ideally, one would spin up the system for several thousand years [*Doney et al.*, 2006] with interglacial orbital parameters (for example 126 kya), and then continue the simulation for another 9 ky with changing orbital parameters until 115 kya is reached. This is too expensive: a 100 year simulation of the present model on the NCAR supercomputers takes about 10 days. Alternatively, one could shorten the spin-up time, and change the orbital parameters from 126 kya to 115 kya within one model time step. This will lead to transients as the model adjusts to the new forcing, and more importantly, the 115 kya part will inherit the result of the long-term model drift from the previous 126 kya part. Even in well tuned GCMs this drift can be to the order of 1°C/kya in the thermocline [*Collins et al.*, 2006], so that the differences between the 126 kya part and the 115 kya part will not be due to orbital forcing alone. Thus, we decided on the present approach of comparing two quasi-equilibrium simulations with identical initial conditions and different orbital parameters. The main drawback of this approach is that in full equilibrium the global net air-sea carbon fluxes have to be identical and zero in both simulations. Thus, it would not be possible to assess whether different orbital forcing leads to different net global fluxes. However, the simulations are not in perfect equilibrium, but for every single 100 year interval the global net air-sea fluxes of carbon show a larger outgassing in OP115 than in CONT (a minimum difference of 0.008 Pg/yr for years 101–200, and a maximum difference of 0.042 Pg/yr for years 201–300; Figure 2). This suggests that the present experimental setup, while not perfect, will still allow us to draw meaningful conclusions about a possible change of air-sea carbon fluxes in response to changes in orbital forcing.

[10] It should be emphasized that the present experiments are not designed to simulate a glacial inception. Rather, their purpose is to demonstrate that at least one full GCM can produce a large Northern Hemisphere response to changes in orbital forcing without the need of additional tuning or flux corrections. This is arguably an important test for GCMs that are used to study climate change. Neither are the experiments designed to reproduce the observed evolution of atmospheric CO_2 concentration: atmospheric CO_2 is fixed to the same value in all experiments, and so is the land cover. Instead, the experiments are designed to quantify the physical
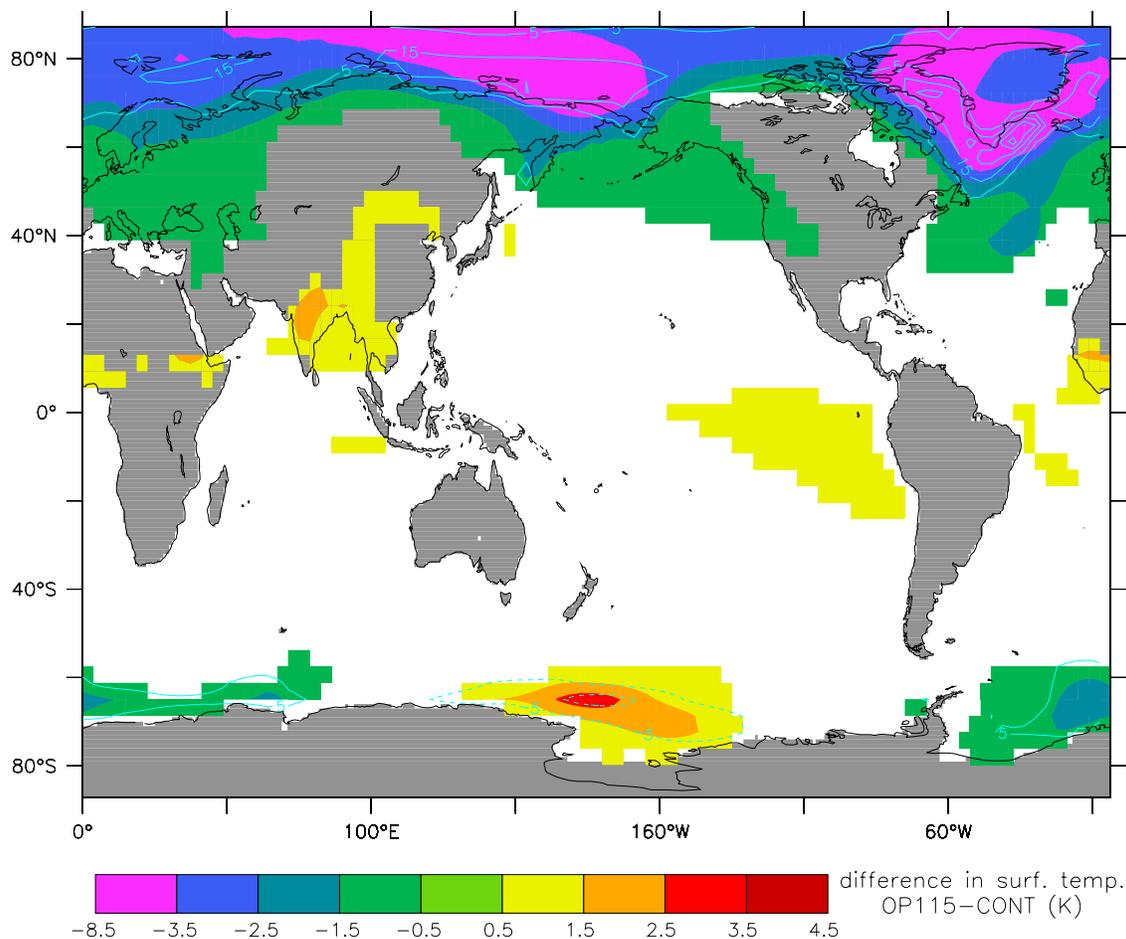
Figure 3. Difference in annual mean surface air temperature and sea ice concentration (color interval 10%) between CONT and OP115 (OP115-CONT). Maximum cooling and maximum increase in sea ice concentration are both southeast of Greenland, with values of 8.5°C and 45%, respectively.

processes that could modify air-sea carbon fluxes during times with different orbital parameters: SST, winds, and sea ice.

3. Results

[11] The insolation differences lead to noticeable differences in climate (Figure 3): strong northern high-latitude cooling with increased sea ice formation, and tropical warming. While the latter is consistent with a larger mean insolation (Figure 1, right), the high-latitude response is not; it is much larger in northern than in southern high latitudes. Interestingly, strength and pattern of the response is similar to the response found by *Vellinga and Wood* [2002]. They perturb the North Atlantic surface salinity by 2 practical salinity units (psu) and find a large Northern Hemisphere cooling and a collapsing of the Atlantic Meridional Overturning Circulation (MOC). Here, too, the changes can be attributed to the strength of the Atlantic Meridional Overturning Circulation (MOC), which is reduced from 14 Sv in CONT to 9 Sv in OP115. The way the experiment is designed it must be concluded that the insolation induced

cooling causes a weakening of the MOC. This is somewhat counterintuitive since the MOC strength is closely linked to the meridional density gradient [e.g., *Bryan*, 1987; *Marotzke*, 1997], and the high-latitude cooling in OP115 should strengthen the MOC. A closer look at the results, however, reveals that the temperature changes are more than compensated for by the salinity changes (Figure 4). This salinity change cannot be accounted for precipitation changes, since it rains less in OP115 than in CONT (not shown). It turns out that the salinity changes are dominated by sea ice dynamics. For the present purpose these can be summarized as follows: sea ice is formed in the Arctic ocean and exported through the Fram and Denmark straits into the North Atlantic. This sea ice or freshwater export is equivalent to a salt import and leads to freshening of the North Atlantic and a salinification of the Arctic (for a recent review of the current freshwater budget of the Arctic see *Dickson et al.* [2007]). Because of the insolation induced cooling this process is amplified in OP115, and the increased Arctic sea ice production and export leads to increased salinification in the Arctic and increased freshening in the North Atlantic (Figure 4). This North Atlantic freshwater cap in OP115
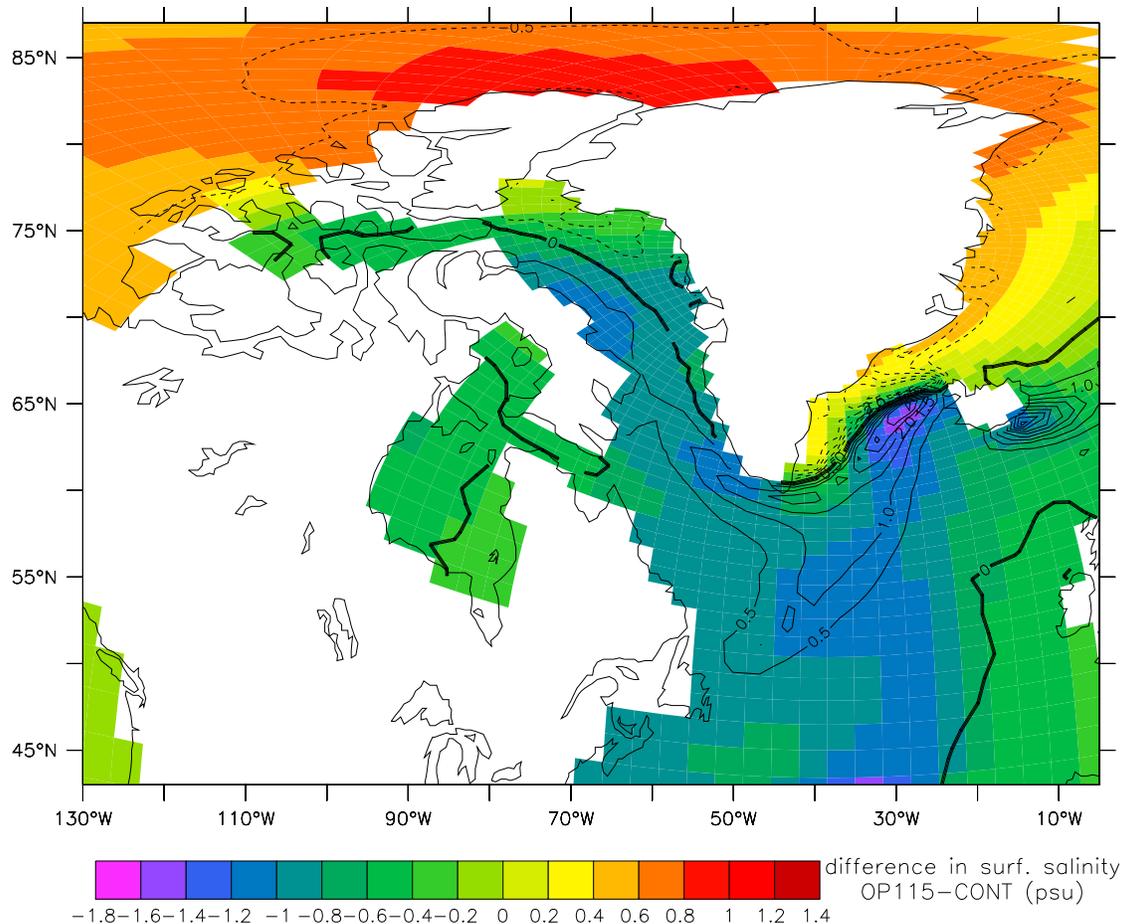
Figure 4. Difference in annual mean sea surface salinity (in psu) and meltwater flux (contour interval 0.5 m/yr) between OP115 and CONT (OP115-CONT). Negative meltwater fluxes indicate net production of sea ice: seawater is frozen, advected away as low-salinity sea ice, and saltier water is left behind.

increases stratification, reduces convection, and subsequently weakens the MOC. To our knowledge this process has not received much attention yet in the discussion of glacial inception. There are observations, however, that explain much of the last century of Arctic temperature variability with solar variability [*Soon*, 2005], and at least one GCM study suggests that present-day MOC variability can partly be explained by variability in Arctic sea ice export [*Jungclaus et al.*, 2005]. Furthermore, sediment core records indicate that the last glacial inception has indeed been accompanied by a freshening of the North Atlantic [*Cortijo et al.*, 1999].

[12] There are several other numerical studies on the last glacial inception; none of which, however, finds that the Atlantic MOC is significantly reduced or is a major link between insolation changes and glaciation: Upon changing the orbital parameters from 126 kya to 115 kya, *Crucifix and Loutre* [2002] find a reduction of maximum MOC strength 5%, *Khodri et al.* [2001] find no change, *Khodri et al.* [2003] find a reduction of 5% if the insolation changes are accompanied by additional freshwater forcing, *Wang and Mysak* [2002] find an increase of 20%, and *Gröger et al.* [2007] find an increase of 5%. With the exception of

Gröger et al. [2007], who use a full, but flux-corrected GCM, these studies are done with models of intermediate complexity. Because they resolve less details of ocean, atmosphere, and sea ice physics than the present primitive-equation GCM, they can be integrated for longer times, and account for other important processes like ice sheet or vegetation feedbacks [e.g., *Calov et al.*, 2005a, 2005b]. Instead of the present MOC feedback, these studies mostly attribute the major insolation amplification to snow-albedo and ice sheet feedbacks. Thus, we see the present results as complimentary to these earlier results, and therefore the sea ice-MOC feedback as relevant as the snow, land ice and vegetation feedbacks.

[13] The temperature changes in Figure 3 are model results, but there are several observations available to validate them. The cooler northern high latitudes 115 kya are recorded in ice core records [e.g., *Schmitt et al.*, 1995], and the 1°C warmer eastern equatorial Pacific is consistent with the analysis of sediment cores by *Lea et al.* [2006]. Furthermore, the Arabian Sea summer monsoon is stronger in CONT than in OP115 (not shown), which is supported by ocean sediment based multiproxy records [*Clemens and Prell*, 2003]. For the 115 kya epoch in the Southern
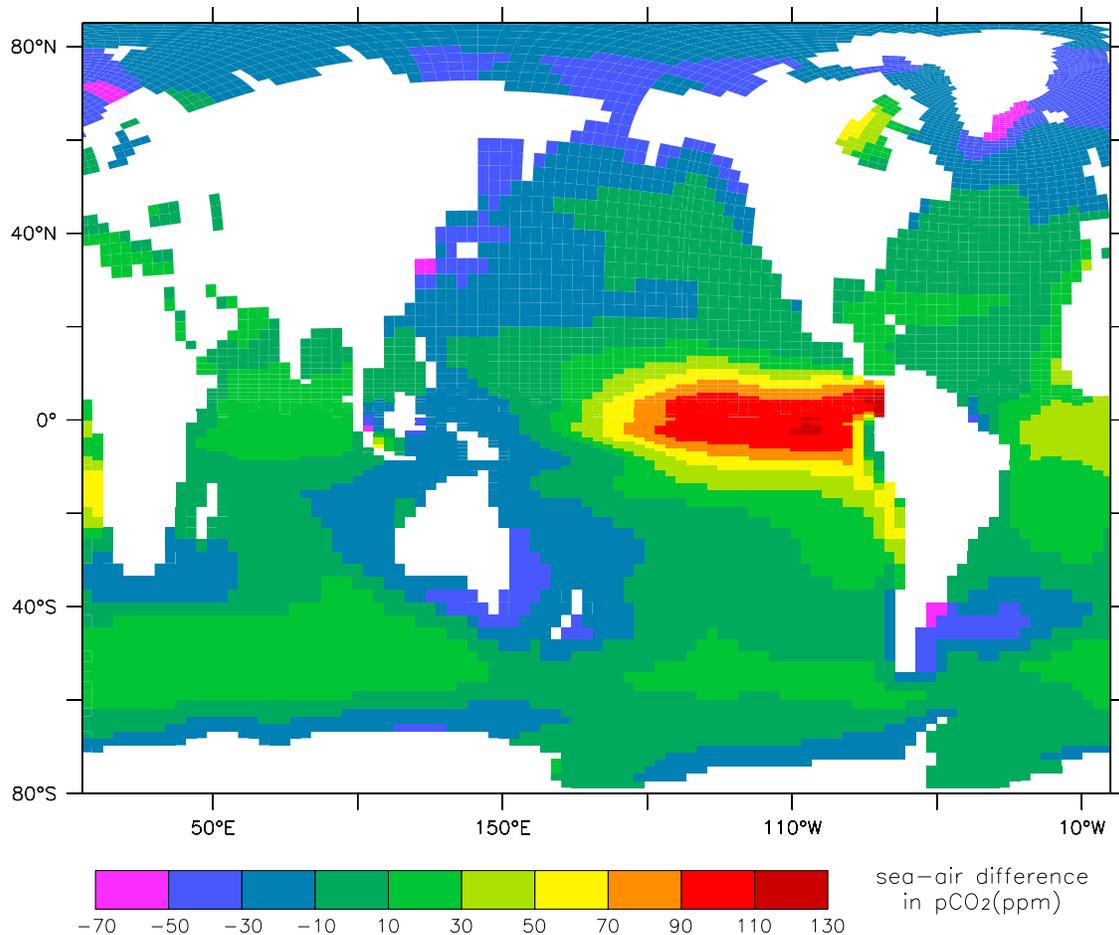
Figure 5. Mean air-sea difference in pCO_2 at the ocean surface in CONT (in ppm).

Ocean there are a few alkenone based SST observations available, all of which support the result of a largely similar SST between OP115 and CONT [*Ikehara et al.*, 1997; *Pahnke and Sachs*, 2006]. One subsurface data set comes from *Stott et al.* [2000], who show, based on carbon isotopes in sediment cores off California, that during the first half of the last ice age the water between 1000 and 2000 meter depth was probably anoxic. Therefore, the Pacific Intermediate water production between 120 kya and 60 kya must have been less than today's. Our experiments, too, show that the oxygen content in this region is reduced, albeit only by 5%–10%. This is similar to the results of the model study by *Gröger et al.* [2007], who report an oxygen reduction of less than 10%. They speculate that the relatively small reduction compared to the observations may be due to the unresolved topography in their coarse resolution OGCM, an argument that would apply here as well. The present simulations carry ideal age, an artificial tracer that indicates when the water was last exposed to the atmosphere. Interestingly, this ideal age tracer shows the water in OP115 to be slightly younger than in CONT (approximately 340 versus 350 years). The formation processes of Pacific Intermediate water is beyond the scope of this manuscript, but this result shows that at

least in CCSM it can be misleading to equate oxygen concentrations with ventilation rates in a linear manner.

[14] The one area where it is beyond doubt that OP115 does not match the observations is Antarctica. The Vostok ice core records indicate that 115 kya it was much cooler than today [e.g., *Petit et al.*, 1999], whereas the experiment shows only little difference between CONT and OP115. However, given the small annual mean insolation differences between CONT and OP115 (Figure 1, right), and the even smaller radiation differences at the surface (not shown), the magnitude of the modeled response is reasonable. Therefore, we proceed with the working hypothesis that the lack of a southern high-latitude response is an indication that during glacial inception it lags the northern high latitudes. The process by which the two polar regions are connected is beyond the scope of the present study, although it can be speculated that drawdown of atmospheric CO_2 by a chemical or biological process that is not present in CCSM is exactly that process. To our knowledge the current observations do not allow to distinguish which hemisphere leads during glacial inception.

[15] It is worthwhile emphasizing here again that it is not attempted to simulate a glacial inception; the model does not
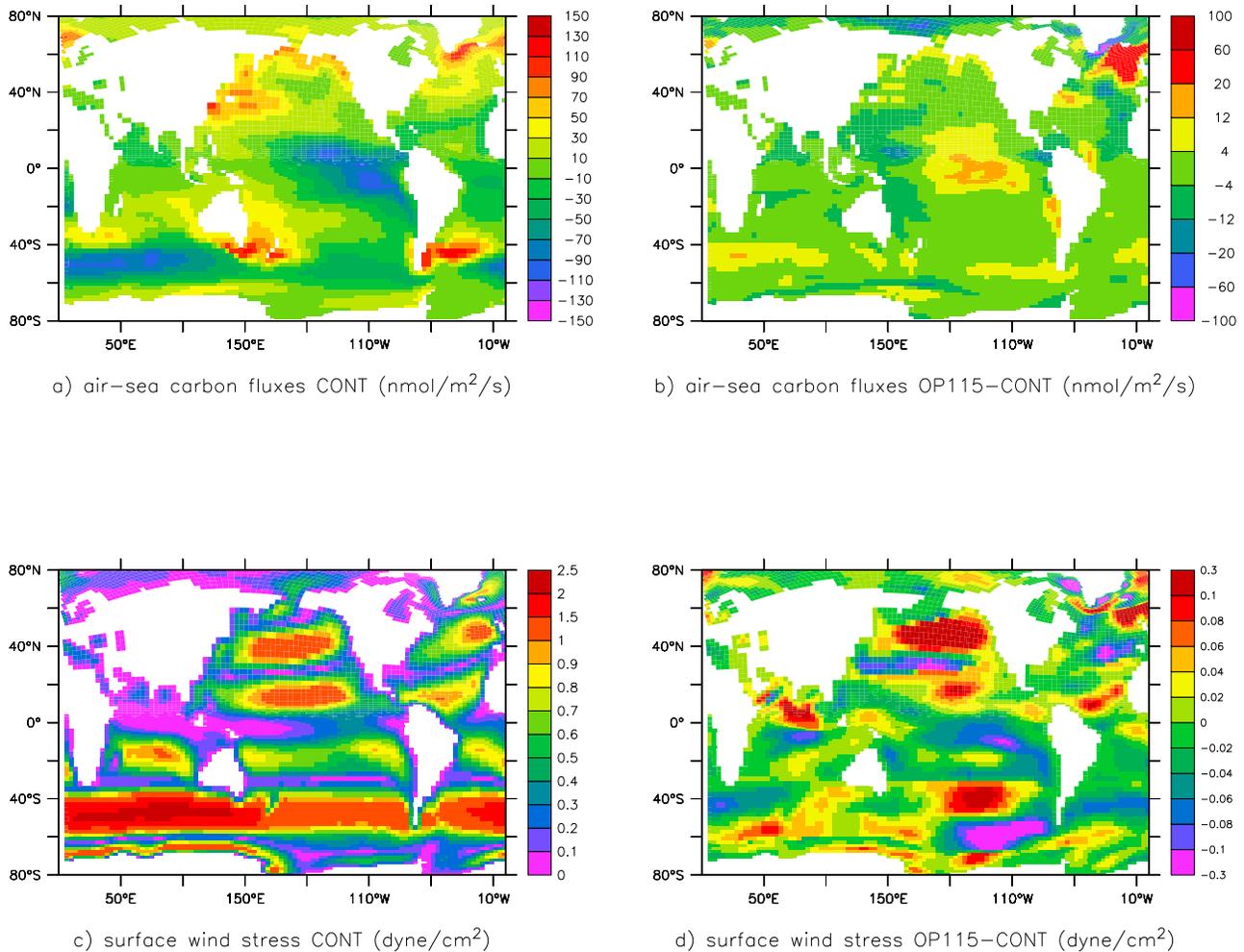
a) air−sea carbon fluxes CONT (nmol/m²/s)

b) air−sea carbon fluxes OP115−CONT (nmol/m²/s)

c) surface wind stress CONT (dyne/cm²)

d) surface wind stress OP115−CONT (dyne/cm²)

Figure 6. (a) Air-sea fluxes of CO_2 CONT and (b) its difference to OP115 (in nmol/m²/s carbon; negative fluxes indicate outgassing) and (c) the absolute surface wind stress CONT and (d) its difference to OP115 (in dyn/cm²). Note that the color intervals are nonequidistant so that equatorial and high-latitude changes can be illustrated in the same image.

simulate ice sheets and is too expensive to be integrated for millennia. Rather, the goal is to understand the initial global response of air-sea CO_2 fluxes to insolation changes. This should provide a small piece to solve the larger puzzle of CO_2 evolution during the last several hundred millennia.

[16] The list of parameters and observable variables in the BEC model is extensive and optimizing a global simulation requires considerable resources and skill [e.g., *Gnanadesikan et al.*, 2004; *Doney et al.*, 2009]. Given these challenges, the annual mean air-sea differences of pCO_2 ($dpCO_2$) are surprisingly close to the observations (compare color plate 3 of *Sarmiento and Gruber* [2006] with Figure 5). In both the maximum pressure difference is in the eastern equatorial Pacific, and the minimum in the deep convection regions of the North Atlantic. In both the Southern Ocean is characterized by large-scale but relatively weak $dpCO_2$. The most notable difference between CONT and the observations is the model's lack of structure in the Indian Ocean (presumably because the coastal upwelling along the Somali coast is not

resolved), and the absence of a large scale negative $dpCO_2$ in the observations of the southern Southern Ocean. However, the Southern Annular Mode [e.g., *Hartmann and Lo*, 1998] can cause large fluctuations in $dpCO_2$ [*Le Quere et al.*, 2000], and the anthropogenic signal in $dpCO_2$, which is present in the observations but absent in CONT, is bound to have a relatively larger ($dpCO_2$ reducing) impact in the Southern Ocean.

[17] Quantitative assessment of export production (downward flux of carbon in particulate matter) and CO_2 air-sea fluxes show that the model is in reasonable agreement with the observations, but slightly overestimates the CO_2 uptake in the polar northern latitudes at the expense of uptake in the temperate Southern Ocean (Table 1). The fluxes in OP115, though, yield a major surprise: in spite of the vastly different physical climate, they are not very different from the fluxes in CONT. It turns out that the three main mechanisms to modify the solubility pump, sea ice, SST and wind, balance each other to inhibit net change. The three regions that show

Table 1. Uptake and Outgassing of CO_2 Across Different Latitude Bands[a]

	Observations	CONT	OP115	IRONCONT
49°N–90°N	0.1	0.387 ± 0.001	0.390 ± 0.001	0.377 ± 0.001
18°N–49°N	0.5	0.404 ± 0.002	0.375 ± 0.002	0.367 ± 0.002
18°S–18°N	−0.7	−0.847 ± 0.007	−0.860 ± 0.007	−0.95 ± 0.009
44°S–18°S	0.6	0.320 ± 0.002	0.324 ± 0.002	0.257 ± 0.002
90°S–44°S	−0.4	−0.432 ± 0.004	−0.424 ± 0.004	−0.422 ± 0.004
90°S–90°N	0.0	−0.168 ± 0.008	−0.194 ± 0.008	−0.366 ± 0.009
Export production	5–15	8.9	8.5	10.0

[a]Positive values are for uptake, and negative values are for outgassing. Values are in Pg/yr. Observations are from *Gruber et al.* [2009], and model results show mean and its standard deviation for years 300–500. For export production, the observations are based on the review by *Oschlies* [2001], and the model values for export production are based on the maximum flux of particulate organic matter (in all runs at 70 m depth). For orientation, the ice core records suggest that the maximum decline in atmospheric CO_2 concentration is approximately 50 ppm over 10,000 years, which translates into 0.01 Pg/yr.

the largest changes in air-sea carbon fluxes are the northern North Atlantic and Arctic Ocean, the equatorial Pacific Ocean, and the Southern Ocean. The changes in carbon flux are to the order of 10%–20% in the latter two, and even up to 100% in the first region (compare Figures 6a and 6b). Thus, there are clearly significant regional differences in the air-sea carbon flux, although the net difference is negligible. This is consistent with the results of *Gröger et al.* [2007], who find no significant change in the atmospheric CO_2 concentration in a transient simulation from 126 kya to 115 kya. Interestingly, theirs is a study with a fully interactive land model, and freely evolving atmospheric CO_2. Thus, in their model all the carbon that the land vegetation loses through insolation induced cooling is taken up by the oceans, which is further evidence that the ocean controls the atmospheric CO_2 concentration. The following discussion of the differences in the present simulations are all based on Figure 6 (unless noted otherwise). The purpose of this discussion is not give a complete account and explanation of all the regional changes; instead it shall highlight the complexity of the different responses and give the reader a general sense of the relative importance of different regions.

[18] The North Atlantic and Arctic oceans are significantly colder, which should enhance the CO_2 uptake, but the cooling is colocated with increased sea ice cover which inhibits air-sea exchange (Figure 3) [see also *Stephens and Keeling*, 2000; *Archer et al.*, 2003]. In particular the area between Greenland, Norway and England shows large changes. This is an area of convection and deep water formation [e.g., *Warren*, 1981], and the increased sea ice concentration in OP115 forces the maximum carbon uptake southward (compare Figure 3 with Figures 6a and 6b) without any net effect (Table 1).

[19] The response in the central to eastern equatorial Pacific is controlled by the warming in the eastern Pacific (Figure 3), which leads to an eastward shift of precipitation (not shown), a weakening of the equatorial westerlies and the associated reduced upwelling and outgassing along the equator (Figure 6b). However, Figure 6 also shows that this basin wide shift in the wind field leads to reduced downwelling and uptake off northeast Australia and increased outgassing in the northern warm pool, the net result of which is, again, almost zero (Table 1).

[20] The westerlies to the south of Africa were weaker in OP115 and shifted south (Figure 6d), which reduces outgassing over this sector. This response lies at the heart of the

theories that link Southern Ocean outgassing with insolation changes and atmospheric CO_2 concentration [e.g., *Toggweiler et al.*, 2006]. However, this particular response happens only over a small part of the Southern Ocean, in other parts the changes to the wind and carbon fluxes are minor so that the total difference is rather small (Table 1). This is consistent with the results of the modeling studies by *Menviel et al.* [2008] and *Tschumi et al.* [2008], who both conclude that changes of the Southern Ocean westerlies cannot be responsible for the interglacial to glacial drop in the atmospheric CO_2 concentration.

[21] It turns out that the only latitudes with a sizable difference in air-sea carbon fluxes are the northern midlatitudes. The cooler Northern Hemisphere in OP115 leads to northward shift of the westerlies over the northern Pacific and Atlantic oceans, and an intensification of the Atlantic northeast trades (Figure 6d). This leads to shifts in the ocean upwelling and downwelling pattern and strength. The carbon flux differences are dominated by the Atlantic, where OP115 has a weaker, but more northward separating Gulf Stream than CONT, as well as stronger coastal upwelling along West Africa (not shown). As in the other domains these changes are largely compensating, but not quite, and they add up to a net difference between OP115 and CONT. Contrary to expectations, though, the carbon uptake is smaller in OP115 than in CONT, and this explains most of the difference seen in the global net difference (Table 1). Limiting the analysis in Table 1 to isopycnals that outcrop in the polar deep water formation regions ($\sigma > 27 \text{ kg/m}^3$) leads to the same conclusion.

[22] Although CCSM is a state of the art GCM, there are biases, misrepresented physics and biogeochemistry; and missing processes like, for example, changes in aeolian dust flux. To illustrate the size of the uncertainties associated with the biogeochemistry, one experiment is added to Table 1 (IRONCONT): It is identical to CONT, except for a different iron sediment source: CONT uses the default iron source from CCSM3, IRONCONT uses the new iron source which will be part of the future CCSM4 release, and includes recently discovered iron sources such as the one off the coast of Papua New Guinea. The differences between the 2 simulations can be interpreted as the uncertainty in the model state resulting from the limited knowledge of sediment iron sources [*Moore and Braucher*, 2008]. Compared to CONT, IRONCONT has an approximately 50% larger chlorophyll concentration in the iron limited regions of the

tropical Pacific, an almost identical mean climate, and a slightly weaker El Niño (see *Jochum et al.* [2010] for a more detailed description). The new iron source leads to larger export production and tropical outgassing, and smaller southern midlatitude CO_2 uptake (Table 1). Since this changes the relative importance of the different domains with respect to the carbon cycle, in can be expected that the net response to a change in orbital parameters is different than in the CONT setup.

4. Summary and Discussion

[23] Several 500 yearlong fully coupled GCM simulations with active ocean ecosystem have been analyzed to quantify the effect of solar insolation on climate and ocean carbon uptake. It is found that insolation changes impact the MOC through modification of generation and export of the Arctic sea ice. This Arctic sea ice link therefore acts to amplify changes in orbital forcing. The differences in Northern Hemisphere climate lead to large regional differences in air-sea carbon fluxes due to differences in sea ice cover, SST and wind stress, but the global or even the basin wide integrals do only change little. If anything, the OP115 scenario has larger outgassing than the CONT scenario.

[24] The results of the IRONCONT simulation demonstrate that the CO_2 flux differences between CONT and OP115 are quite small compared to flux differences arising from model uncertainties. Thus, the solubility pump as an important component of the CO_2 response to orbital forcing cannot be discarded completely. One possible way forward would be to treat this as a probabilistic problem, and compute the flux differences from a large set of CONT-OP115 couples, each with reasonable but different physical and biological parameters. The range of answers would allow to establish a confidence level for the response. This path requires a fast technique to reach equilibrium, which is cur-

rently being developed and will hopefully evolve into a standard component of CCSM [e.g., *Kwon and Primeau*, 2006].

[25] Another possibility is that the modeled air-sea carbon fluxes are realistic, but that the vegetation response to the combined orbital forcing and MOC changes significantly modifies climate and air-sea fluxes beyond the presently described differences. This is quite possible [e.g., *Gallimore and Kutzbach*, 1996], and even the present configuration with fixed vegetation shows OP115 cooler than CONT in Europe and Siberia (Figure 3). A natural next step is then to repeat the current set of experiments with interactive vegetation, which will be focus of our future research.

[26] Regarding the simulated connection between insolation, Arctic sea ice production and the MOC, it is important to repeat the simulations with the new generation of high-resolution coupled models. Running these GCMs with the full ocean ecosystem is still out of reach, but since this process is independent of biology or chemistry it can be assessed in a computationally much less expensive physics-only configuration. There is no reason to believe that the present T31x3 configuration of CCSM has an unphysical response to orbital forcing variations. However, the potential implications of this process, if it really occurred in past epochs, are large and deserve to be investigated with a GCM that really resolves the boundary currents around Greenland and the flow into the convection regions of the North Atlantic.

References

Archer, D. E., P. A. Martin, J. Milovich, V. Brovkin, G.-K. Plattner, and C. Ashendel (2003), Model sensitivity in the effect of Antarctic sea ice and stratification on atmospheric pCO_2, *Paleoceanography*, 18(1), 1012, doi:10.1029/2002PA000760.

Berger, A., and M. F. Loutre (1991), Insolation values for the climate of the last 10,000,000 years, *Quat. Sci. Rev.*, 10, 297–317.

Berger, A. L., and P. Pestiaux (1984), Accuracy and stability of the Quaternary terrestrial insolation, in *Milankovitch and Climate*, edited by A. Berger et al., pp. 83–111, D. Reidel, Dordrecht, Netherlands.

Bryan, F. O. (1987), Parameter sensitivity of primitive ocean circulation models, *J. Phys. Oceanogr.*, 17, 970–985.

Calov, R., A. Ganopolski, M. Claussen, V. Petoukhov, and R. Greve (2005a), Transient simulation of the last glacial inception. Part I: Glacial inception as a bifurcation in the climate system, *Clim. Dyn.*, 24, 545–561.

Calov, R., A. Ganopolski, V. Petoukhov, M. Claussen, V. Brovkin, and C. Kubatzki (2005b), Transient simulation of the last glacial inception. Part II: Sensitivity and feedback analysis, *Clim. Dyn.*, 24, 563–576.

Clemens, S. C., and W. L. Prell (2003), A 350,000 year summer-monsoon multi-proxy stack from the Owen Ridge, northern Arabian Sea, *Mar. Geol.*, 201, 35–51.

Collins, W. D., et al. (2006), The Community Climate System Model version 3 (CCSM3), *J. Clim.*, 19, 2122–2143.

Cortijo, E., S. Lehman, L. Keigwin, M. Chapman, D. Paillard, and L. Labeyrie (1999), Changes in meridional temperature and salinity gradients in the North Atlantic Ocean (30°–72°N) during the last interglacial period, *Paleoceanography*, 14, 23–33.

Crucifix, M., and M. F. Loutre (2002), Transient simulations over the last interglacial period (126–115 kyr BP): Feedback and forcing analysis, *Clim. Dyn.*, 19, 417–433.

Dickson, R., B. Rudels, S. Dye, M. Karcher, J. Meincke, and I. Yashayaev (2007), Current estimates of freshwater flux through Arctic and subarctic seas, *Prog. Oceanogr.*, 73, 210–230.

Doney, S. C., I. Lima, K. Lindsay, J. K. Moore, S. Dutkiewicz, M. A. M. Friedrichs, and R. J. Matear (2001), Marine biogeochemical modeling: Recent advances and future challenges, *Oceanography*, 14, 93–107.

Doney, S. C., K. Lindsay, I. Fung, and J. John (2006), Natural variability in a stable, 1000-yr global coupled climate-carbon cycle simulation, *J. Clim.*, 19, 3033–3054.

Doney, S. C., I. Lima, J. K. Moore, K. Lindsay, M. J. Behrenfeld, T. K. Westberry, N. Mahowald, D. M. Glover, and T. Takahashi (2009), Skill metrics for confronting global upper ocean ecosystem-biogeochemistry models against field and remote sensing data, *J. Mar. Syst.*, 76, 95–112.

Gallimore, R. G., and J. E. Kutzbach (1996), Role of orbitally induced changes in tundra area in the onset of glaciation, *Nature*, 381, 503–505.

Gnanadesikan, A., J. P. Dunne, R. M. Key, K. Matsumoto, J. L. Sarmiento, R. D. Slater, and P. S. Swathi (2004), Oceanic ventilation and biogeochemical cycling: Understanding the physical mechanisms that produce realistic distributions of tracers and productivity, *Global Biogeochem. Cycles*, 18, GB4010, doi:10.1029/2003GB002097.

Gröger, M., E. Maier-Reimer, U. Mikolajewicz, G. Schurgers, M. Vizcaíno, and A. Winguth (2007), Changes in the hydrological cycle, ocean circulation, and carbon/nutrient cycling during the last interglacial and glacial transi-

tion, *Paleoceanography*, *22*, PA4205, doi:10.1029/2006PA001375.

Gruber, N., et al. (2009), Oceanic sources, sinks, and transport of atmospheric CO$_2$, *Global Biogeochem. Cycles*, *23*, GB1005, doi:10.1029/2008GB003349.

Hartmann, D. L., and F. Lo (1998), Wave-driven zonal flow vacillation in the Southern Hemisphere, *J. Atmos. Sci.*, *55*, 1303–1315.

Hays, J. D., J. Imbrie, and N. J. Shackleton (1976), Variations in the Earth's orbit: Pacemaker of the ice ages, *Science*, *194*, 1121–1132.

Huybers, P., and E. Tziperman (2008), Integrated summer insolation forcing and 40,000-year glacial cycles: The perspective from an ice-sheet/energy-balance model, *Paleoceanography*, *23*, PA1208, doi:10.1029/2007PA001463.

Huybers, P., and C. Wunsch (2004), A depth-derived Pleistocene age model: Uncertainty estimates, sedimentation variability, and nonlinear climate change, *Paleoceanography*, *19*, PA1028, doi:10.1029/2002PA000857.

Ikehara, M., K. Kawamura, N. Ohkouchi, K. Kimoto, M. Murayama, T. Nakamura, T. Oba, and A. Taira (1997), Alkenone sea surface temperature in the Southern Ocean for the last two deglaciations, *Geophys. Res. Lett.*, *24*, 679–682.

Jochum, M. (2009), Impact of latitudinal variations in vertical diffusivity on climate simulations, *J. Geophys. Res.*, *114*, C01010, doi:10.1029/2008JC005030.

Jochum, M., S. Yeager, K. Lindsay, K. Moore, and R. Murtugudde (2010), Quantification of the feedback between phytoplankton and ENSO in the Community Climate System Model, *J. Clim.*, *23*, 2916–2925.

Jungclaus, J. H., H. Haak, M. Latif, and U. Mikolajewicz (2005), Arctic–North Atlantic interactions and multidecadal variability of the meridional overturning circulation, *J. Clim.*, *18*, 4013–4030.

Khodri, M., Y. Leclainche, G. Ramstein, P. Braconnot, O. Marti, and E. Cortijo (2001), Simulating the amplification of orbital forcing by ocean feedbacks in the last glaciation, *Nature*, *410*, 570–574.

Khodri, M., G. Ramstein, D. Paillard, J. C. Duplessy, M. Kageyama, and A. Ganopolski (2003), Modelling the climate evolution from the last interglacial to the start of the last glaciation: The role of Arctic Ocean freshwater budget, *Geophys. Res. Lett.*, *30*(12), 1606, doi:10.1029/2003GL017108.

Knox, F., and M. McElroy (1984), Changes in atmospheric CO$_2$: Influence of marine biota at high latitudes, *J. Geophys. Res.*, *89*, 4629–4637.

Kwon, E. Y., and F. Primeau (2006), Optimization and sensitivity study of a biogeochemistry ocean model using an implicit solver and in situ phosphate data, *Global Biogeochem. Cycles*, *20*, GB4009, doi:10.1029/2005GB002631.

Lane, E., S. Peacock, and J. Restrepo (2006), A dynamic-flow carbon-cycle box model and high-latitude sensitivity, *Tellus, Ser. B*, *58*, 257–278.

Lea, D. W., D. K. Pak, C. L. Belanger, H. J. Spero, M. A. Hall, and N. J. Shackleton (2006), Paleoclimate history of Galápagos surface waters over the last 135,000 yr, *Quat. Sci. Rev.*, *25*, 1152–1167.

Le Quere, C., J. C. Orr, P. Monfray, O. Aumont, and G. Madec (2000), Interannual variability of the oceanic sink of CO$_2$ from 1979 to 1997, *Global Biogeochem. Cycles*, *14*, 1247–1265.

Marotzke, J. (1997), Boundary mixing and the dynamics of the three-dimensional thermohaline circulations, *J. Phys. Oceanogr.*, *27*, 1713–1728.

Menviel, L., A. Timmermann, A. Mouchet, and O. Timm (2008), Climate and marine carbon cycle response to changes in the strength of the Southern Hemispheric westerlies, *Paleoceanography*, *23*, PA4201, doi:10.1029/2008PA001604.

Milankovitch, M. (1941), *Kanon der Erdbestrahlung und seine Auswirkung auf das Eiszeitenproblem*, *R. Serbian Acad. Sci. Spec. Publ.*, vol. 132, 633 pp., Isr. Program for Sci. Transl., Jerusalem.

Moore, J. K., and O. Braucher (2008), Sedimentary and mineral dust sources of dissolved iron to the world ocean, *Biogeosciences*, *5*, 631–656.

Moore, J. K., S. C. Doney, J. A. Kleypas, D. M. Glover, and I. Y. Fung (2001), An intermediate complexity marine ecosystem model for the global domain, *Deep Sea Res., Part II*, *49*, 403–462.

Moore, J. K., S. C. Doney, and K. Lindsay (2004), Upper ocean ecosystem dynamics and iron cycling in a global three-dimensional model, *Global Biogeochem. Cycles*, *18*, GB4028, doi:10.1029/2004GB002220.

Oschlies, A. (2001), Model-derived estimates of new production: New results point towards lower values, *Deep Sea Res., Part II*, *48*, 2173–2197.

Pahnke, K., and J. P. Sachs (2006), Sea surface temperatures of southern midlatitudes 0–160 kyr B.P., *Paleoceanography*, *21*, PA2003, doi:10.1029/2005PA001191.

Peacock, S., E. Lane, and J. M. Restrepo (2006), A possible sequence of events for the generalized glacial-interglacial cycle, *Global Biogeochem. Cycles*, *20*, GB2010, doi:10.1029/2005GB002448.

Petit, J. R., et al. (1999), Climate and atmospheric history of the past 420,000 years from the Vostok ice core, Antarctica, *Nature*, *399*, 429–436.

Sarmiento, J. L., and N. Gruber (2006), *Ocean Biogeochemical Dynamics*, Princeton Univ. Press, Princeton, N. J.

Sarmiento, J. L., and J. R. Toggweiler (1984), A new model for the role of oceans in determining atmospheric CO$_2$, *Nature*, *308*, 621–624.

Schmitt, F., S. Lovejoy, and D. Schertzer (1995), Multifractal analysis of the Greenland ice-core project climate data, *Geophys. Res. Lett.*, *22*, 1689–1692.

Short, D. A., J. G. Mengel, T. J. Crowley, W. T. Hyde, and G. R. North (1991), Filtering of Milankovitch cycles by Earth's geography, *Quat. Res.*, *35*, 157–173.

Siegenthaler, U., and T. Wenk (1984), Rapid atmospheric CO$_2$ variations and ocean circulation, *Nature*, *308*, 624–626.

Sigman, D. M., and E. A. Boyle (2000), Glacial/interglacial changes in atmospheric carbon dioxide, *Nature*, *407*, 859–869.

Soon, W. W.-H. (2005), Variable solar irradiance as a plausible agent for multidecadal variations in the Arctic-wide surface air temperature record of the past 130 years, *Geophys. Res. Lett.*, *32*, L16712, doi:10.1029/2005GL023429.

Stephens, B. B., and R. F. Keeling (2000), The influence of Antarctic sea ice on glacial-interglacial CO$_2$ variations, *Nature*, *145*, 171–174.

Stott, L. D., M. Neumann, and D. Hammond (2000), Intermediate water ventilation on the northeastern Pacific margin during the late Pleistocene inferred from benthic foraminiferal δ^{13}C, *Paleoceanography*, *15*, 161–169.

Toggweiler, J. R., A. Gnanadesikian, S. Carson, R. Murnane, and J. L. Sarmiento (2003), Representation of the carbon cycle in box models and GCMs: 1. Solubililty pump, *Global Biogeochem. Cycles*, *17*(1), 1026, doi:10.1029/2001GB001401.

Toggweiler, J. R., J. L. Russell, and S. R. Carson (2006), Midlatitude westerlies, atmospheric CO$_2$, and climate change during the ice ages, *Paleoceanography*, *21*, PA2005, doi:10.1029/2005PA001154.

Tschumi, T., F. Joos, and P. Parekh (2008), How important are Southern Hemisphere wind changes for low glacial carbon dioxide? A model study, *Paleoceanography*, *23*, PA4208, doi:10.1029/2008PA001592.

Vellinga, M., and R. A. Wood (2002), Global climatic impacts of a collapse of the Atlantic thermohaline circulation, *Clim. Change*, *54*, 251–267.

Wang, Z., and L. A. Mysak (2002), Simulation of the last glacial inception and rapid ice sheet growth in the McGill Paleoclimate Model, *Geophys. Res. Lett.*, *29*(23), 2102, doi:10.1029/2002GL015120.

Warren, B. A. (1981), Deep circulation of the world ocean, in *Evolution of Physical Oceanography*, edited by B. A. Warren and C. Wunsch, pp. 6–41, MIT Press, Cambridge, Mass.

Yeager, S. G., C. A. Shields, W. G. Large, and J. J. Hack (2006), The low-resolution CCSM3, *J. Clim.*, *19*, 2545–2566.

M. Jochum, K. Lindsay, and S. Peacock, National Center for Atmospheric Research, Boulder, CO 80305, USA. (markus@ucar.edu; klindsay@ucar.edu; synte@ucar.edu)

K. Moore, Department of Earth System Science, University of California, Irvine, CA 92697, USA. (jkmoore@uci.edu)